

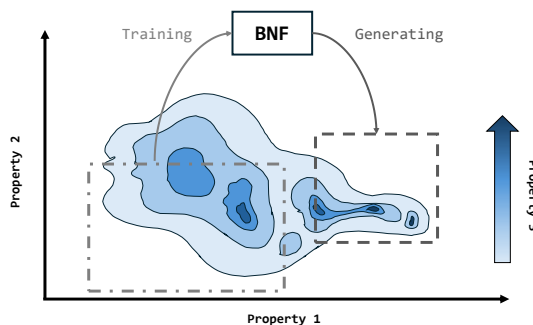
Bayesian Flow Is All You Need to Sample Out-of-Distribution Chemical Spaces

Nianze TAO

Department of Chemistry, Graduate School of Advanced Science and Engineering,
Hiroshima University, 1-3-1 Kagamiyama, Higashi-Hiroshima, Japan 739-8524
tao-nianze@hiroshima-u.ac.jp

Abstract

Generating novel molecules with higher properties than the training space, namely the out-of-distribution generation, is important for *de novo* drug design. However, it is not easy for distribution learning-based models, for example diffusion models, to solve this challenge as these methods are designed to fit the distribution of training data as close as possible. In this paper, we show that Bayesian flow network is capable of effortlessly generating high quality out-of-distribution samples that meet several scenarios. We introduce a semi-autoregressive training/sampling method that helps to enhance the model performance and surpass the state-of-the-art models.



1 Introduction

The chemical space is large, and even the sub-space is too large to be explored completely. For instance, the number of *small* drug-like molecules is believed to be over 10^{60} ,¹⁻³ amongst which, however, only a much smaller sub-region, e.g., macrocycles,⁴⁻⁶ were tested in the laboratories and applied into real world challenges; when we start considering larger systems like proteins, the space grows exponentially.⁷

Recent emerging deep generative models that virtually search the chemical space are attractive alternatives to trial-and-error processes conducted by human scientists.⁸⁻¹² Despite the success of generative models, especially the distributional learning models, in molecule generation, some researchers have pointed out the limitations of these methods: because the models and benchmarks were designed to optimise and test the in-distribution performance, i.e., how *close* the generated molecules are to the training data, (1) the models were poor at generating highly novel samples with desired properties;^{9,13} (2) multi-objective optimisation was difficult;⁹ (3) the sampling space could change to the false-positive region volatily when an overconfident guidance appeared.¹⁴ To overcome these problems, it is important to improve the performance of out-of-distribution (OOD) generation, i.e., generating compounds with higher properties than that of molecules in the training dataset.

Pioneering works have introduced a few methods to enhance the diffusion models' OOD performance including introducing a dedicatedly designed control method to steer towards the OOD

space,⁹ and utilising unlabelled data to increase the training domain and regularise the model.¹⁴ In this research, we, on the other hand, show that the Bayesian flow network, another branch of deep generative methods, is a *natural* out-of-distribution sampler. Moreover, we demonstrate that by introducing a semi-autoregressive behaviour our method outperform several state-of-the-art (SOTA) models in OOD multi-objective optimisation tasks.

2 Methods

2.1 Bayesian Flow Networks

Similar to denoising diffusion models^{15–17} (DMs), Bayesian flow networks¹⁸ (BFNs) splits the generative process to a sequential steps. Some research has pointed out that the generative process of BFN is similar to thus can be approximated as a reversed stochastic differential equation (SDE) though,^{19,20} BFN method does not require to define a diffusion process nor learns the noise distribution: instead, BFN directly optimises the parameters of a distribution towards a more informative direction, which makes it applicable to continuous, discretised, and discrete data as the *parameters* of any real-world distribution is continuous.¹⁸ The previous studies have already applied the idea of BFN to 3-dimensional molecular conformation generation^{21,22} (discretised and continuous case), text-based molecule generation²³ (discrete case), and protein sequence generation²⁰ (discrete case), which proved its capability of understanding the chemical space. In this research, we employ ChemBFN,²³ a BFN model handling the 1-dimensional molecular representation originally designed to generate SMILES²⁴ and SELFIES²⁵ strings, to study BFN’s potentials of out-of-distribution sampling, i.e., generating samples with high properties out of a low-property training space. We show that a small change in the training or sampling process of ChemBFN can significantly enhance the out-of-distribution generative performance.

2.2 Semi-autoregressive Training and Sampling

In the original ChemBFN²³ model and any BERT²⁶-like model, tokens are updated bidirectionally as illustrated in Figure 1 (left), where for an arbitrary token in a finite fixed-length sequence $s_j \in (s_0, s_1, s_2, \dots, s_N)$ a function f_{BI} maps s_j from i^{th} layer to $(i+1)^{th}$ layer based on itself and tokens from both left side (previous tokens) and right side (subsequent tokens), i.e., $s_j^{i+1} = f_{BI}(s_j^i; s_{0:j-1}^i, s_{j+1:N}^i)$. In the case of autoregressive models, however, since the sequence is extended step by step (as shown in Figure 1 (middle)), the next token s_{j+1} only comes from the previous tokens via a function f_{AR} , i.e., $s_{j+1}^{i+1} = f_{AR}(s_{0:j}^i)$. For models employing self-attention mechanism, e.g., the decoder of autoencoder transformer²⁷ model and GPT²⁸ model, a causal mask that maps entities of the attention matrix above the main diagonal to zero is applied to implement this autoregressive behaviour. We found that in a trained ChemBFN model, the entities that were far away from the main diagonal in the attention matrices were extremely close to zero, which enlightened the possibility of applying causal masks to ChemBFN models without breaking models’ generative capability. By employing the causal mask, we introduce a semi-autoregressive (SAR) behaviour to ChemBFN models, in which all tokens are updated together as a block but subsequent tokens are not used to update the current token (Figure 1 (right)), i.e., $s_j^{i+1} = f_{SAR}(s_j^i; s_{0:j-1}^i)$.

To be simple, we denote applying causal masks to models as ‘SAR’ while ‘normal’ stands for disabling causal masks. Depending on whether the causal masks are used in training or sampling processes, four strategies (strategy 1 - 4) are proposed in Table 1. We show how these settings affect the generative behaviours of our model in later texts.

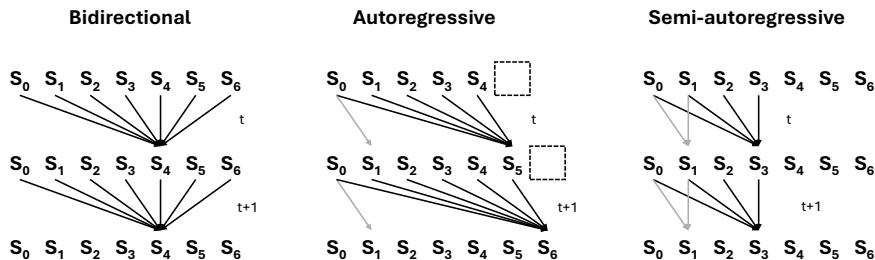


Figure 1: Visualisation of bidirectional, autoregressive, and semi-autoregressive token update methods.

Table 1: Training and sampling strategies. SAR stands for ‘semi-autoregressive’.

Strategy	Training	Sampling
1	normal	normal
2	normal	SAR
3	SAR	normal
4	SAR	SAR

2.3 Datasets and Benchmarks

MOSES²⁹ is a widely-used benchmark in the studies of small molecule generation. Apart from testing the validity, uniqueness, diversity, and novelty of generated molecules, this benchmark focuses more on the distribution learning performances of tested models, including Tanimoto similarity (SNN), fragment similarity (Frag), scaffold similarity (Scaf), and Fréchet ChemNet Distance³⁰ (FCD). Although the purpose of MOSES is to estimate how *close* the learnt distribution is to the training space, in the study it was utilised to showcase how *far away* the generated space of our method could be from the training space while retaining the chemical meaningfulness.

Lee *et al.*,⁹ on the other hand, proposed ZINC250k dataset, which is consisted of 249,455 molecules collected from ZINC³¹ database and their paired quantitative estimate of drug-likeness³² (QED), synthetic accessibility³³ (SA), and docking scores (DS) unit in kcal/mol to five different proteins (PARP1, FA7, 5HT1B, BRAF, and JAK2) calculated via QuickVina 2,³⁴ and the corresponding metrics to test the OOD multi-objective guided molecular generating performance. In this benchmark, a group of filters that should be applied to generated molecules are defined as

$$\begin{cases} \text{QED} > 0.5 \\ \text{SA} < 5 \\ \text{DS} < \widetilde{\text{DS}}(\text{molecules in training data}) \\ \text{SNN} < 0.4, \end{cases} \quad (1)$$

where $\widetilde{\text{DS}}$ stands for median value of docking score and SNN is the Margon fingerprint Tanimoto similarity to the nearest neighbour in the training set. The two metrics, *novel hit ratio* and *novel*

top 5% docking score, are therefore defined as

$$\begin{cases} \text{Novel hit ratio} & = \frac{N^{\text{e}} \text{ molecules passed all the filters}}{N^{\text{e}} \text{ generated molecules}} \times 100\% \\ \text{Novel top 5\% docking score} & = \overline{DS}(\text{top 5\% molecules passed all the filters}). \end{cases} \quad (2)$$

According to Lee *et al.*,⁹ it is recommended to sample 3,000 molecules for each target protein and to repeat the experiment for 5 times to obtain the mean and standard deviation of the metrics.

Apart from studying the small molecule generating, we further employed a labelled protein dataset (90,990 sequences in the training set) published by N. Gruver *et al.*³⁵ to test our method on the generative tasks of larger systems. Amongst several structure-related labels, we selected the percentage of beta sheets and solvent accessible surface area (SASA) as the objective targets as suggested by N. Gruver *et al.*³⁵

3 Experiments and Results

We first demonstrated how different training and sampling strategies defined in Section 2.2 affected generated spaces of unconditional cases, then quantified the performance of our model in OOD multi-object optimisations.

3.1 Unconditional Generation of Small Molecules

The MOSES testing metrics of ChemBFN using different strategies were visualised in Figure 2 and the 2-dimensional UMAP³⁶ plots of unconditional sample spaces of models trained on ZINC250k dataset against the training space were shown in Figure 3. It is clear that diversity and structure related metrics did not significantly response to the change of training and/or sampling strategies, which indicated that SAR process did not worsen the model’s capability of learning molecular structures. The key observation was that the OOD-ness indicated by the magnitude of FCD was strongly affected by different strategies. Figure 3 and Figure 5 (a) further showed that the sample spaces were *far away* from the training space while changing training and/or sampling strategies led the model to explore different OOD spaces.

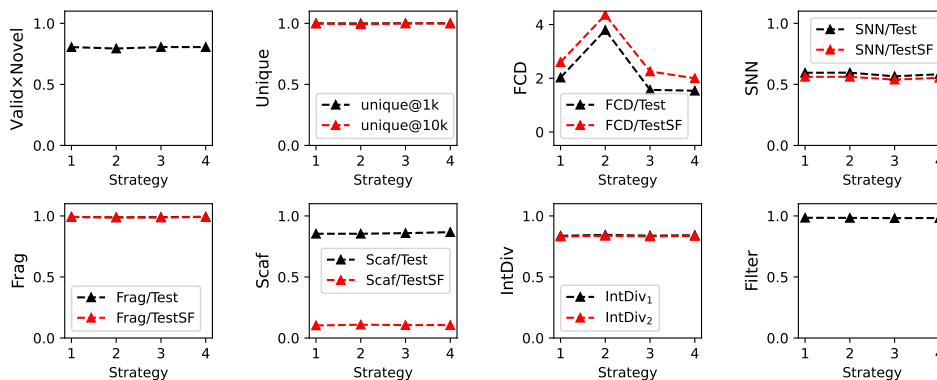


Figure 2: Visualisation of MOSES benchmark metrics of different strategies. We reported Valid x Novel values instead of validity and novelty separately.

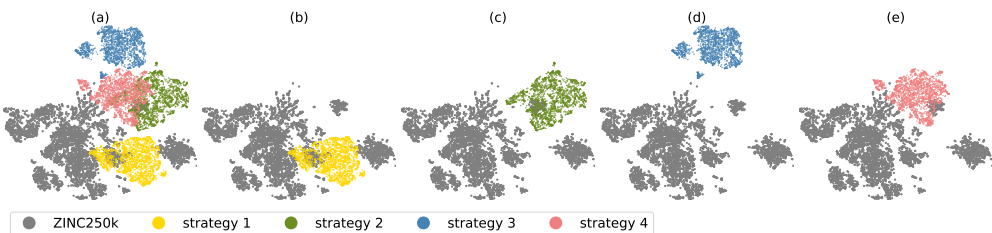


Figure 3: UMAP visualisation of the training space of ZINC250k dataset and the unconditionally generated sample spaces of different strategies.

3.2 Conditional Generation of Small Molecules

When a guidance vector $\mathbf{y} = (\text{QED}, \text{SA}, \text{DS})$ pointing to a higher-property space than training space, i.e., high drug-likeness, low synthetic difficulty and more negative docking affinity, was applied to the sampling process via the classifier-free guidance method,³⁷ we observed that the sample spaces had a tendency to be close to each other regardless the change of strategy (Figure 4). The OOD-ness was significantly larger than unconditional cases (Figure 5).

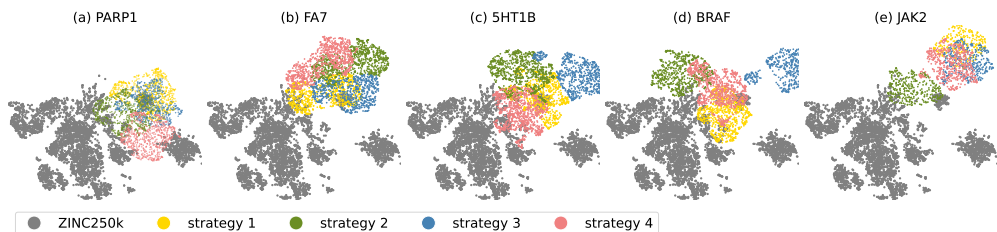


Figure 4: UMAP visualisation of the training space of ZINC250k dataset and the conditionally generated sample spaces of different strategies.

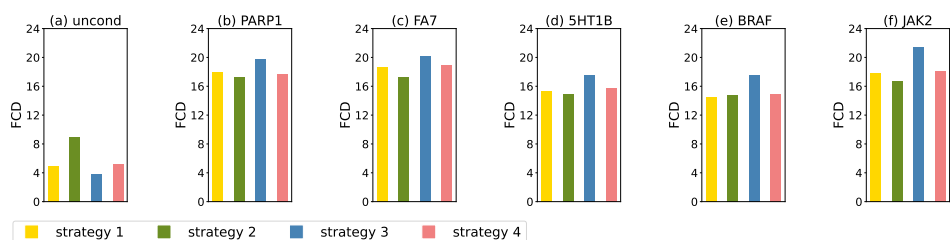


Figure 5: FCD values of unconditional and conditional samples of different strategies.

In Table 2 and Table 3, we summarised the novel hit ratios and novel top 5% docking scores of ChemBFN when different training and/or sampling strategies were applied compared with the SOAT models^{9,38–42} (note that the data of the SOTA models were provided by Lee et al⁹). Regarding to the novel hit ratio, ChemBFN coupled with strategy 4 gave the best results on 4 out of 5 tasks amongst ChemBFN family, which, however, only outperformed the best method on 2 out of 5 tasks. Conversely, all our models outperformed all the SOTA methods for all 5

tasks when concerning the novel top 5% docking scores, amongst which ChemBFN coupled with strategy 3 showed the best performance and strategy 4 presented the second best results.

Table 2: Novel hit ratios (\uparrow) compared with SOTA models. The best results are in **bold** and the second best results are underlined. We sampled the molecules for 1,000 steps in **SMILES** format. The results were the average values of 5 runs with the standard deviation reported.

Methods	PARP1	FA7	Target proteins 5HT1B	BRAF	JAK2
REINVENT ³⁸	0.480 \pm 0.344	0.213 \pm 0.081	2.453 \pm 0.561	0.127 \pm 0.088	0.613 \pm 0.167
MORLD ³⁹	0.047 \pm 0.050	0.007 \pm 0.013	0.880 \pm 0.735	0.047 \pm 0.040	0.227 \pm 0.118
HierVAE ⁴⁰	0.553 \pm 0.214	0.007 \pm 0.013	0.507 \pm 0.278	0.207 \pm 0.220	0.227 \pm 0.127
FREED ⁴¹	3.627 \pm 0.961	1.107 \pm 0.209	<u>10.187</u> \pm 3.306	2.067 \pm 0.626	4.520 \pm 0.673
GDSS ⁴²	1.933 \pm 0.208	0.368 \pm 0.103	4.667 \pm 0.306	0.167 \pm 0.134	1.167 \pm 0.281
MOOD ⁹	7.017 \pm 0.428	0.733 \pm 0.141	18.673 \pm 0.423	5.240 \pm 0.285	9.200 \pm 0.524
ChemBFN strategy 1	5.040 \pm 0.473	<u>5.827</u> \pm 0.475	3.100 \pm 0.264	5.340 \pm 0.341	3.973 \pm 0.253
ChemBFN strategy 2	4.660 \pm 0.302	5.567 \pm 0.153	3.653 \pm 0.248	<u>5.293</u> \pm 0.529	4.040 \pm 0.240
ChemBFN strategy 3	4.287 \pm 0.303	4.520 \pm 0.383	3.860 \pm 0.089	3.160 \pm 0.314	4.093 \pm 0.368
ChemBFN strategy 4	<u>5.593</u> \pm 0.417	5.853 \pm 0.423	4.587 \pm 0.358	4.233 \pm 0.518	<u>5.260</u> \pm 0.314

Table 3: Novel top 5% docking scores (\downarrow) compared with SOTA models. The best results are in **bold** and the second best results are underlined. We sampled the molecules for 1,000 steps in **SMILES** format. The results were the average values of 5 runs with the standard deviation reported.

Methods	PARP1	FA7	Target proteins 5HT1B	BRAF	JAK2
REINVENT ³⁸	-8.702 \pm 0.523	-7.205 \pm 0.264	-8.770 \pm 0.316	-8.392 \pm 0.400	-8.165 \pm 0.277
MORLD ³⁹	-7.532 \pm 0.260	-6.263 \pm 0.165	-7.869 \pm 0.650	-8.040 \pm 0.337	-7.816 \pm 0.133
HierVAE ⁴⁰	-9.487 \pm 0.278	-6.812 \pm 0.274	-8.081 \pm 0.252	-8.978 \pm 0.525	-8.285 \pm 0.370
FREED ⁴¹	-10.427 \pm 0.177	-8.297 \pm 0.094	-10.425 \pm 0.331	-10.325 \pm 0.164	-9.624 \pm 0.102
GDSS ⁴²	-9.967 \pm 0.028	-7.775 \pm 0.039	-9.459 \pm 0.101	-9.224 \pm 0.068	-8.926 \pm 0.089
MOOD ⁹	-10.865 \pm 0.113	-8.160 \pm 0.071	-11.145 \pm 0.042	-11.063 \pm 0.034	-10.147 \pm 0.060
ChemBFN strategy 1	<u>-12.932</u> \pm 0.159	-9.186 \pm 0.149	-12.493 \pm 0.313	-11.955 \pm 0.143	-11.792 \pm 0.337
ChemBFN strategy 2	-12.528 \pm 0.205	-8.925 \pm 0.083	-11.912 \pm 0.265	-11.728 \pm 0.103	-11.677 \pm 0.169
ChemBFN strategy 3	-13.040 \pm 0.211	-9.611 \pm 0.154	<u>-12.448</u> \pm 0.241	-12.350 \pm 0.641	-12.111 \pm 0.275
ChemBFN strategy 4	-12.741 \pm 0.205	<u>-9.442</u> \pm 0.074	-12.275 \pm 0.120	<u>-11.969</u> \pm 0.203	<u>-12.022</u> \pm 0.120

We found that when a guidance vector pointing to a higher-property space than training space is applied, the ratio of invalid SMILES²⁴ strings generated by the models increased drastically. To remove the influence of hallucinations, we additionally trained two models (ChemBFN + strategy 3 and ChemBFN + strategy 4 as they performed the best amongst ChemBFN family) to generate SELFIES²⁵ strings. The results were shown in Table 4 and Table 5. The novel hit ratio for all target proteins, as shown in Table 4, significantly improved from less than 6% to over 25%, which outperformed all the SOTA models. The novel top 5% docking scores dropped slightly as shown in Table 5. Nevertheless, our models still surpassed SOTA methods.

Table 4: Novel hit ratios (\uparrow) compared with SOTA models. The best results are in **bold** and the second best results are underlined. We sampled the molecules for 1,000 steps in **SELFIES** format. The results were the average values of 5 runs with the standard deviation reported.

Methods	PARP1	FA7	Target proteins 5HT1B	BRAF	JAK2
REINVENT ³⁸	0.480 \pm 0.344	0.213 \pm 0.081	2.453 \pm 0.561	0.127 \pm 0.088	0.613 \pm 0.167
MORLD ³⁹	0.047 \pm 0.050	0.007 \pm 0.013	0.880 \pm 0.735	0.047 \pm 0.040	0.227 \pm 0.118
HierVAE ⁴⁰	0.553 \pm 0.214	0.007 \pm 0.013	0.507 \pm 0.278	0.207 \pm 0.220	0.227 \pm 0.127
FREED ⁴¹	3.627 \pm 0.961	1.107 \pm 0.209	10.187 \pm 3.306	2.067 \pm 0.626	4.520 \pm 0.673
GDSS ⁴²	1.933 \pm 0.208	0.368 \pm 0.103	4.667 \pm 0.306	0.167 \pm 0.134	1.167 \pm 0.281
MOOD ⁹	7.017 \pm 0.428	0.733 \pm 0.141	18.673 \pm 0.423	5.240 \pm 0.285	9.200 \pm 0.524
ChemBFN strategy 3	31.547 \pm 0.73	31.460 \pm 0.858	25.047 \pm 0.837	26.893 \pm 1.022	34.06 \pm 0.710
ChemBFN strategy 4	33.240 \pm 1.018	<u>30.133</u> \pm 0.442	30.933 \pm 0.573	29.033 \pm 0.647	42.133 \pm 1.509

Table 5: Novel top 5% docking scores (\downarrow) compared with SOTA models. The best results are in **bold** and the second best results are underlined. We sampled the molecules for 1,000 steps in **SELFIES** format. The results were the average values of 5 runs with the standard deviation reported.

Methods	PARP1	FA7	Target proteins 5HT1B	BRAF	JAK2
REINVENT ³⁸	-8.702 \pm 0.523	-7.205 \pm 0.264	-8.770 \pm 0.316	-8.392 \pm 0.400	-8.165 \pm 0.277
MORLD ³⁹	-7.532 \pm 0.260	-6.263 \pm 0.165	-7.869 \pm 0.650	-8.040 \pm 0.337	-7.816 \pm 0.133
HierVAE ⁴⁰	-9.487 \pm 0.278	-6.812 \pm 0.274	-8.081 \pm 0.252	-8.978 \pm 0.525	-8.285 \pm 0.370
FREED ⁴¹	-10.427 \pm 0.177	-8.297 \pm 0.094	-10.425 \pm 0.331	-10.325 \pm 0.164	-9.624 \pm 0.102
GDSS ⁴²	-9.967 \pm 0.028	-7.775 \pm 0.039	-9.459 \pm 0.101	-9.224 \pm 0.068	-8.926 \pm 0.089
MOOD ⁹	-10.865 \pm 0.113	-8.160 \pm 0.071	-11.145 \pm 0.042	-11.063 \pm 0.034	-10.147 \pm 0.060
ChemBFN strategy 3	-12.455 \pm 0.068	-9.527 \pm 0.033	-12.609 \pm 0.045	<u>-12.043</u> \pm 0.117	-11.690 \pm 0.105
ChemBFN strategy 4	<u>-12.358</u> \pm 0.102	<u>-9.315</u> \pm 0.026	<u>-12.359</u> \pm 0.172	-12.061 \pm 0.087	<u>-11.666</u> \pm 0.089

Examples of novel hit molecules generated by our model (both SMILES version and SELFIES version) were illustrated in Figure 6 and Figure 7. An interesting observation is that although the ring systems in the training data are generally small, our model tended to generate larger ring systems or even macrocyclic systems that showed lower binding energies.

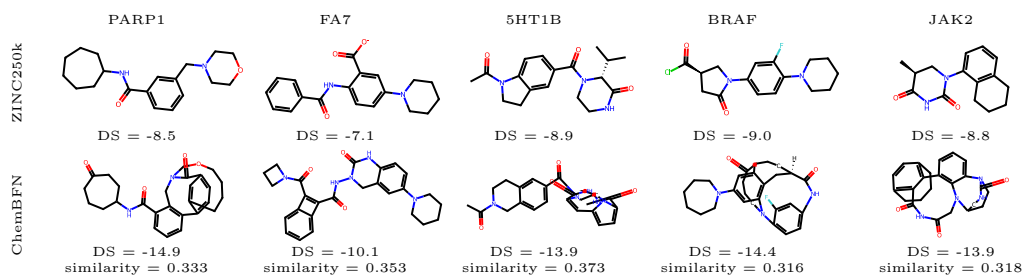


Figure 6: Examples of novel hit molecules generated by ChemBFN (**SMILES** version) against their closest neighbours in the training space.

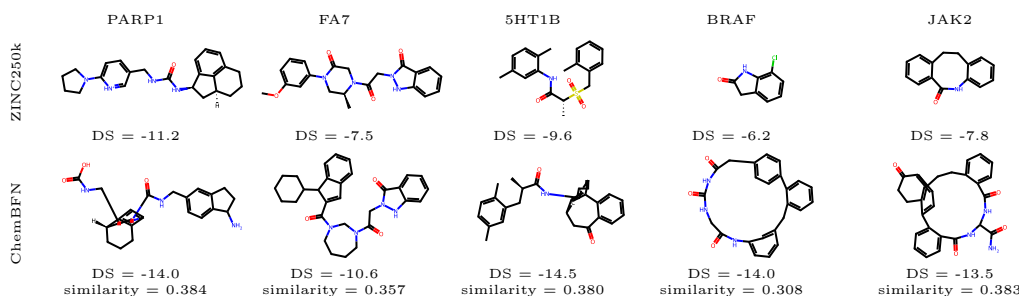


Figure 7: Examples of novel hit molecules generated by ChemBFN (**SELFIES** version) against their closest neighbours in the training space.

3.3 Conditional Generation of Protein Sequences

An amino acid tokenizer was added to the original ChemBFN model to enable protein sequence generating. We trained one model to optimise the percentage of beta sheets and one model to optimise SASA. Each model, after training, generated 32×2 protein sequences (half was generated via strategy 3 and half via strategy 4) guided by an objective value pointing to the high property regions. As shown in Figure 8, the generated samples all had higher objective values than the training space. When estimated the naturalness (ProtGPT2⁴³ log likelihood as suggested by N. Gruver *et al*³⁵) of the generated proteins, we found that models utilising either strategy 3 or strategy 4 gave reasonably acceptable results compared with natural proteins (see Figure 8). As SASA and the percentage of beta sheets of proteins are highly correlated their structures, we conclude that our model is capable of determining the relationship between an objective (scalar) value to its corresponding chemical structures, unsupervised, and extrapolating to unseen spaces.

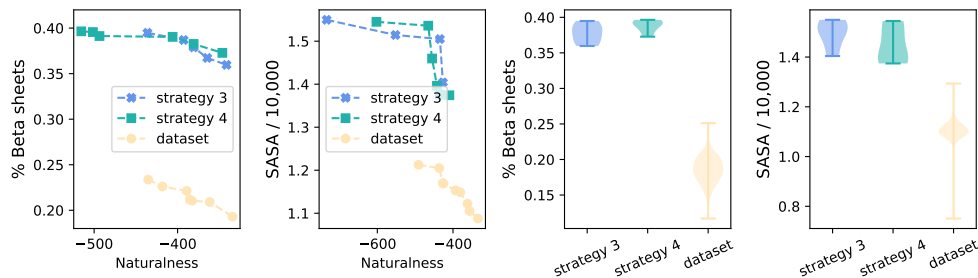


Figure 8: (Left 2 plots) The Pareto fronts of objective values *v.s.* naturalness of generated protein sequences and dataset; (Right 2 plots) The violin plots of the objective values of generated samples and dataset. Notice that our method generated proteins with higher objective values than any entity in the training dataset while maintaining the similar naturalness to natural proteins.

3.4 What If You Care More About In-Distribution Sampling

In this section, we demonstrate how pre-training affects the sampling distributions of MOSES as an example. Finetuned models based on models, provided by N. Tao *et al*,²³ pretrained on 40M and 190M molecules selected from ZINC15 database⁴⁴ were denoted as ‘finetuned 1’ and ‘finetuned 2’, respectively. As shown in Figure 9, the increasing of pre-training data surprisingly

led to the decrease of FCD metrics. However, when applying LoRA⁴⁵ finetune strategy (rank = 4, $\alpha = 1$) to the pretrained model (pretrained on 190M molecules), both FCD and the ratio of novel generated molecules increased while the ratio of molecules which passed the MOSES benchmark filters decreased. We conclude here that larger scale pre-training helps to obtain generated molecules closer to the training space only when all the parameters of the network were finetuned; on the other hand, LoRA finetuning, i.e., reduced parameter finetuning, will further strengthen the OOD-ness.

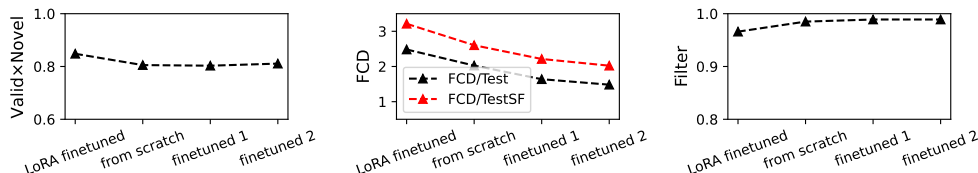


Figure 9: The key MOSES testing metrics of finetuned models. We reported Valid \times Novel values instead of validity and novelty separately. Note that we employed strategy 1 in this experiment.

3.5 Computational Details

All the models were trained on single Nvidia A100 GPU with a batch-size of 120 for MOSES dataset and 128 for ZINC250k dataset for 100 epochs. The learning rate was 5×10^{-5} which was linearly increased from 10^{-8} during the first 1,000 steps. AdamW⁴⁶ method with default parameters was employed to optimise the model weights. A unconditional rate of 0.2 was chosen when training conditional models. During sampling process, the batch-size was 3,000 for small molecules and 32 for protein sequences; the guidance strength was 0.5 for small molecules and 1.0 for protein sequences when a guidance vector was applied. The number of sampling steps was 100 for MOSES and 1,000 for ZINC250k and protein sequences. The models trained for generating small molecules had 12 layers, 8 attention heads per layer and 512 hidden feature sizes (54.5M of total parameters); the models for protein sequences had 12 layers, 16 attention heads per layer and 1,024 hidden feature sizes (216M of total parameters).

RDKit⁴⁷ was used to generate 3-dimensional conformations and Morgan fingerprint (radius = 2, dimension = 1024) from SMILES strings and calculate the Tanimoto similarity, QED, and SA quantities. The docking scores were computed via QuickVina 2.³⁴ The properties of proteins were calculate via Biopython⁴⁸ package version 1.84; to obtain the solvent accessible surface area, the 3-dimensional structures were predicted by ESMFold⁴⁹ model first, which was followed by Shrake-and-Rupley algorithm⁵⁰ calculations.

In order to generate UMAP plots, the vector molecular representations were extracted from the last activation layer of ChemNet,³⁰ which were later projected to 2-dimensional vectors by UMAP package.³⁶ 5,000 random molecules were selected from the dataset as the representatives.

4 Conclusion

In this research, we showed that BFN, especially ChemBFN model, is naturally a controllable out-of-distribution sampler, which is versatile to generate both small molecules and large chemical systems such as proteins. We found that for unconditional generation, the normal training-SAR sampling strategy promoted the OOD-ness of the model most; when a guidance was switched on, the OOD behaviour was pushed to a higher level, in which case the SAR trained models out-

performed several state-of-the-art methods: the SAR training-normal sampling strategy tended to samples with higher objective values while the SAR training-SAR sampling strategy had a tendency to yield more novel samples. The generated samples in the OOD regions satisfied several real-world requirements including high drug-likeness, low synthetic difficulties, and similar naturalness to their natural counterparts, which makes our method a strong candidate to handle *de novo* drug design challenges.

5 Data and Software Availability

The code of ChemBFN and instructions necessary to reproduce the results of this study are available for download at <https://github.com/Augus1999/bayesian-flow-network-for-chemistry>.

6 Acknowledgements

The computational source of GPU was provided by Research Center for Computational Science, Okazaki, Japan (Project: 24-IMS-C043).

7 Conflict of Interest

The author claim no conflicts of interest.

8 Funding Sources

The authors claim that there is no funding related to this research.

References

- [1] R. S. Bohacek, C. McMartin and W. C. Guida, *Medicinal research reviews*, 1996, **16**, 3–50.
- [2] P. Ertl, *Journal of chemical information and computer sciences*, 2003, **43**, 374–380.
- [3] J.-L. Reymond, R. van Deursen, L. C. Blum and L. Ruddigkeit, *Med. Chem. Commun.*, 2010, **1**, 30–38.
- [4] E. M. Abdelraheem, S. Shaabani and A. Dömling, *Drug Discovery Today: Technologies*, 2018, **29**, 11–17.
- [5] D. Garcia Jimenez, V. Poongavanam and J. Kihlberg, *Journal of Medicinal Chemistry*, 2023, **66**, 5377–5396.
- [6] E. M. Driggers, S. P. Hale, J. Lee and N. K. Terrett, *Nature Reviews Drug Discovery*, 2008, **7**, 608–624.
- [7] J. Maynard Smith, *Nature*, 1970, **225**, 563–564.
- [8] R. Gómez-Bombarelli, J. N. Wei, D. Duvenaud, J. M. Hernández-Lobato, B. Sánchez-Lengeling, D. Sheberla, J. Aguilera-Iparraguirre, T. D. Hirzel, R. P. Adams and A. Aspuru-Guzik, *ACS central science*, 2018, **4**, 268–276.

- [9] S. Lee, J. Jo and S. J. Hwang, *Exploring Chemical Space with Score-based Out-of-distribution Generation*, 2023, <https://arxiv.org/abs/2206.07632>.
- [10] J. Lim, S. Ryu, J. W. Kim and W. Y. Kim, *Journal of cheminformatics*, 2018, **10**, 31.
- [11] D. Schwalbe-Koda and R. Gómez-Bombarelli, in *Generative Models for Automatic Chemical Design*, Springer International Publishing, 2020, p. 445–467.
- [12] W. Zhung, H. Kim and W. Y. Kim, *Nature Communications*, 2024, **15**, 2688.
- [13] W. P. Walters and M. Murcko, *Nature biotechnology*, 2020, **38**, 143–145.
- [14] L. Klarner, T. G. J. Rudner, G. M. Morris, C. M. Deane and Y. W. Teh, *Context-Guided Diffusion for Out-of-Distribution Molecular and Protein Design*, 2024, <https://arxiv.org/abs/2407.11942>.
- [15] J. Ho, A. Jain and P. Abbeel, *Advances in neural information processing systems*, 2020, **33**, 6840–6851.
- [16] J. Song, C. Meng and S. Ermon, *Denosing Diffusion Implicit Models*, 2022, <https://arxiv.org/abs/2010.02502>.
- [17] J. Sohl-Dickstein, E. Weiss, N. Maheswaranathan and S. Ganguli, Proceedings of the 32nd International Conference on Machine Learning, Lille, France, 2015, pp. 2256–2265.
- [18] A. Graves, R. K. Srivastava, T. Atkinson and F. Gomez, *Bayesian Flow Networks*, 2024, <https://arxiv.org/abs/2308.07037>.
- [19] K. Xue, Y. Zhou, S. Nie, X. Min, X. Zhang, J. Zhou and C. Li, *Unifying Bayesian Flow Networks and Diffusion Models through Stochastic Differential Equations*, 2024, <https://arxiv.org/abs/2404.15766>.
- [20] T. Atkinson, T. D. Barrett, S. Cameron, B. Guloglu, M. Greenig, L. Robinson, A. Graves, L. Copoiu and A. Laterre, *Protein Sequence Modelling with Bayesian Flow Networks*, 2024, <https://www.biorxiv.org/content/early/2024/09/26/2024.09.24.614734>.
- [21] Y. Song, J. Gong, H. Zhou, M. Zheng, J. Liu and W.-Y. Ma, The Twelfth International Conference on Learning Representations, 2024.
- [22] Y. Qu, K. Qiu, Y. Song, J. Gong, J. Han, M. Zheng, H. Zhou and W.-Y. Ma, *MolCRAFT: Structure-Based Drug Design in Continuous Parameter Space*, 2024, <https://arxiv.org/abs/2404.12141>.
- [23] N. Tao and M. Abe, *A Bayesian Flow Network Framework for Chemistry Tasks*, 2024, <https://arxiv.org/abs/2407.20294>.
- [24] D. Weininger, *Journal of chemical information and computer sciences*, 1988, **28**, 31–36.
- [25] M. Krenn, F. Häse, A. Nigam, P. Friederich and A. Aspuru-Guzik, *Machine Learning: Science and Technology*, 2020, **1**, 045024.
- [26] J. Devlin, M.-W. Chang, K. Lee and K. Toutanova, *BERT: Pre-training of Deep Bidirectional Transformers for Language Understanding*, 2019, <https://arxiv.org/abs/1810.04805>.

- [27] A. Vaswani, N. Shazeer, N. Parmar, J. Uszkoreit, L. Jones, A. N. Gomez, L. Kaiser and I. Polosukhin, *Attention Is All You Need*, 2023, <https://arxiv.org/abs/1706.03762>.
- [28] G. Yenduri, R. M. C. S. G, S. Y, G. Srivastava, P. K. R. Maddikunta, D. R. G, R. H. Jhaveri, P. B, W. Wang, A. V. Vasilakos and T. R. Gadekallu, *Generative Pre-trained Transformer: A Comprehensive Review on Enabling Technologies, Potential Applications, Emerging Challenges, and Future Directions*, 2023, <https://arxiv.org/abs/2305.10435>.
- [29] D. Polykovskiy, A. Zhebrak, B. Sanchez-Lengeling, S. Golovanov, O. Tatanov, S. Belyaev, R. Kurbanov, A. Artamonov, V. Aladinskiy, M. Veselov, A. Kadurin, S. Johansson, H. Chen, S. Nikolenko, A. Aspuru-Guzik and A. Zhavoronkov, *Molecular Sets (MOSES): A Benchmarking Platform for Molecular Generation Models*, 2020, <https://arxiv.org/abs/1811.12823>.
- [30] K. Preuer, P. Renz, T. Unterthiner, S. Hochreiter and G. Klambauer, *Journal of Chemical Information and Modeling*, 2018, **58**, 1736–1741.
- [31] J. J. Irwin and B. K. Shoichet, *Journal of chemical information and modeling*, 2005, **45**, 177–182.
- [32] G. R. Bickerton, G. V. Paolini, J. Besnard, S. Muresan and A. L. Hopkins, *Nature chemistry*, 2012, **4**, 90–98.
- [33] P. Ertl and A. Schuffenhauer, *Journal of cheminformatics*, 2009, **1**, 8.
- [34] A. Alhossary, S. D. Handoko, Y. Mu and C.-K. Kwoh, *Bioinformatics*, 2015, **31**, 2214–2216.
- [35] N. Gruver, S. Stanton, N. Frey, T. G. J. Rudner, I. Hotzel, J. Lafrance-Vanasse, A. Rajpal, K. Cho and A. G. Wilson, Proceedings of the 37th International Conference on Neural Information Processing Systems, Red Hook, NY, USA, 2024.
- [36] L. McInnes, J. Healy and J. Melville, *UMAP: Uniform Manifold Approximation and Projection for Dimension Reduction*, 2020, <https://arxiv.org/abs/1802.03426>.
- [37] J. Ho and T. Salimans, *Classifier-Free Diffusion Guidance*, 2022, <https://arxiv.org/abs/2207.12598>.
- [38] M. Olivecrona, T. Blaschke, O. Engkvist and H. Chen, *Journal of cheminformatics*, 2017, **9**, 48.
- [39] W. Jeon and D. Kim, *Scientific reports*, 2020, **10**, 22104.
- [40] W. Jin, D. Barzilay and T. Jaakkola, Proceedings of the 37th International Conference on Machine Learning, 2020, pp. 4839–4848.
- [41] S. Yang, D. Hwang, S. Lee, S. Ryu and S. J. Hwang, *Hit and Lead Discovery with Explorative RL and Fragment-based Molecule Generation*, 2021, <https://arxiv.org/abs/2110.01219>.
- [42] J. Jo, S. Lee and S. J. Hwang, *Score-based Generative Modeling of Graphs via the System of Stochastic Differential Equations*, 2022, <https://arxiv.org/abs/2202.02514>.
- [43] N. Ferruz, S. Schmidt and B. Höcker, *Nature communications*, 2022, **13**, 4348.
- [44] T. Sterling and J. J. Irwin, *Journal of chemical information and modeling*, 2015, **55**, 2324–2337.

- [45] E. J. Hu, Y. Shen, P. Wallis, Z. Allen-Zhu, Y. Li, S. Wang, L. Wang and W. Chen, International Conference on Learning Representations, 2022.
- [46] I. Loshchilov and F. Hutter, *Fixing Weight Decay Regularization in Adam*, 2019, <https://arxiv.org/abs/1711.05101>.
- [47] *RDKit: Open-source cheminformatics*, <https://www.rdkit.org>, Accessed: 2024-11-12.
- [48] P. J. A. Cock, T. Antao, J. T. Chang, B. A. Chapman, C. J. Cox, A. Dalke, I. Friedberg, T. Hamelryck, F. Kauff, B. Wilczynski and M. J. L. de Hoon, *Bioinformatics*, 2009, **25**, 1422–1423.
- [49] Z. Lin, H. Akin, R. Rao, B. Hie, Z. Zhu, W. Lu, N. Smetanin, A. dos Santos Costa, M. Fazel-Zarandi, T. Sercu, S. Candido *et al.*, *Language models of protein sequences at the scale of evolution enable accurate structure prediction*, 2022.
- [50] A. Shrake and J. A. Rupley, *Journal of molecular biology*, 1973, **79**, 351–371.